THERYA, 2023, Vol. 14(1):181-195 DOI:10.12933/therya-23-2243 ISSN 2007-3364

An 1896 specimen helps clarify the phylogenetic placement of the Mexican endemic Hooper's deer mouse

Susette Castañeda-Rico[1, 2, 3]*, Cody W. Edwards[1, 3], Melissa T. R. Hawkins[4], and Jesús E. Maldonado[1, 2, 3]

[1] Smithsonian-Mason School of Conservation, Front Royal, VA, U.S.A. Email: susetteazul@gmail.com, castanedaricos@si.edu (SC-R), cedward7@gmu.edu (CWE), maldonadoj@si.edu (JEM).
[2] Center for Conservation Genomics, Smithsonian National Zoo and Conservation Biology Institute, Washington DC, U.S.A.
[3] Department of Biology, George Mason University, Fairfax, VA, U.S.A.
[4] Department of Vertebrate Zoology, Division of Mammals, National Museum of Natural History, Washington DC, U.S.A. Email: hawkinsmt@si.edu (MTRH).
*Corresponding author: https://orcid.org/0000-0002-4301-3579.

Hooper's deer mouse, *Peromyscus hooperi*, is the sole member of the *Peromyscus hooperi* species group. This species is endemic to México where it is restricted to the grassland transition zone in the states of Coahuila, Zacatecas, and San Luis Potosí. Previous studies using mitochondrial and nuclear genes (*Cytb*, *Adh1-I2*, *Fgb-I7* and *Rbp3*) did not resolve the phylogenetic relationships of this relatively poorly known species. It was hypothesized that *P. hooperi* is sister to *P. crinitus*, and these two taxa are related to *P. melanotis, P. polionotus, P. maniculatus, P. keeni, P. leucopus, P. gossypinus, P. eremicus, P. californicus,* and *Osgoodomys banderanus*. Based on morphological characters, karyotypes, and allozymes, *P. hooperi* does not align with either subgenera *Haplomylomys* or *Peromyscus*. However, its unique characteristics (*e. g.,* phallus, karyotype) have been recognized, and therefore it has been retained as its own species group. To better resolve the phylogenetic placement of *P. hooperi*, we performed target-enrichment and high-throughput sequencing and obtained several thousand nuclear ultraconserved elements and a complete mitogenome from a specimen collected in 1896 by Nelson and Goldman in Coahuila, México. We compared these data with 21 other species of neotomines using genome-wide data. Contrary to previous studies, we found high nodal support for the placement of *P. hooperi* as sister to a clade that includes *Podomys floridanus, Neotomodon alstoni, Habromys simulatus, H. ixtlani, Peromyscus mexicanus, P. megalops, P. melanophrys, P. perfulvus, P. aztecus, P. attwateri, P. pectoralis,* and *P. boylii*. We dated a Pliocene divergence of *P. hooperi* from its sister group at approximately 3.98 mya, and after the split of *P. crinitus* at *ca.* 4.31 mya from other peromyscines. We demonstrated that genome-wide data improve the phylogenetic signal, independently of taxon sampling, for a phylogenetically problematic species such as *P. hooperi*. We recommend that future genomic studies expand taxon sampling, including members of the subgenus *Haplomylomys*, to confirm the phylogenetic relationships of *P. hooperi* and the genetic status of its populations.

El ratón de Hooper *Peromyscus hooperi*, es el único miembro del grupo de especies que lleva su mismo nombre. Es una especie endémica de México que se encuentra restringida a las zonas de transición de pastizales en los estados de Coahuila, Zacatecas y San Luis Potosí. Estudios previos en los que se han analizado genes mitocondriales y nucleares (*Cytb*, *Adh1-I2*, *Fgb-I7* y *Rbp3*) no han podido resolver las relaciones filogenéticas de esta especie poco conocida. Sin embargo, se ha sugerido que *P. hooperi* podría ser la especie hermana de *P. crinitus*, y estar cercanamente relacionada con *P. melanotis, P. polionotus, P. maniculatus, P. keeni, P. leucopus, P. gossypinus, P. eremicus, P. californicus* y *Osgoodomys banderanus*. Con base en datos morfológicos, cariotipos y aloenzimas, no se ha podido determinar si esta especie se encuentra más estrechamente relacionada con el subgénero *Haplomylomys* o *Peromyscus*. Sin embargo, las características únicas de *P. hooperi* (*e. g.,* falo, cariotipo) han sido reconocidas, por lo que se ha mantenido en su propio grupo de especies. Con el objetivo de proveer nueva evidencia sobre la posición filogenética de *P. hooperi*, utilizamos el método de captura por hibridación y secuenciación masiva para obtener miles de elementos ultraconservados y el genoma mitocondrial de un ejemplar colectado en 1896 por Nelson y Goldman en Coahuila, México. Además, analizamos datos genómicos de 21 especies de neotominos. Contrario a estudios previos, encontramos altos valores de soporte en el nodo que posiciona a *P. hooperi* como la especie hermana del clado que incluye a *Podomys floridanus, Neotomodon alstoni, Habromys simulatus, H. ixtlani, Peromyscus mexicanus, P. megalops, P. melanophrys, P. perfulvus, P. aztecus, P. attwateri, P. pectoralis* y *P. boylii*. Datamos la divergencia de *P. hooperi* de su grupo hermano hace aproximadamente 3.98 millones de años, después de la divergencia de *P. crinitus* y de otros peromiscinos hace aproximadamente 4.31 millones de años, ambos eventos durante el Plioceno. Nuestro estudio es un claro ejemplo de que analizar datos a nivel del genoma mejoran la señal filogenética, independientemente del número de taxones, para especies cuyas relaciones filogenéticas son conflictivas o se encuentran poco resueltas como en el caso de *P. hooperi*. Sin embargo, recomendamos que futuros estudios genómicos incluyan un muestreo taxonómico más amplio, sobre todo de miembros del subgénero *Haplomylomys*, para confirmar las relaciones filogenéticas de *P. hooperi* y el estatus genético de sus poblaciones.

Keywords: Historical DNA; genomics; mitogenomes; museum specimens; *Peromyscus*, Pliocene-Pleistocene; ultraconserved elements.

Introduction

Two of the most important naturalists from the turn of the 20th Century were Edward William Nelson and Edward Alphonso Goldman. They contributed greatly to our knowledge, understanding, and documentation of the biota in the United States and México (López-Medellin and Medellin 2016, https://sova.si.edu/record/SIA.FARU7364). The scientific material collected by both naturalists continues to be used as a rich resource in the systematic revision of many groups of birds and mammals (López-Medellin and Medellin 2016). Nelson and Goldman's biological surveys encompassed all of the states in México and lasted 14 years (1892 to 1906). In 1896, Nelson and Goldman conducted field work in Coahuila, México where they collected three individuals, later recognized as *Peromyscus hooperi*. These specimens were deposited and remain housed at the Smithsonian Institution's National Museum of Natural History in Washington DC.

Peromyscus hooperi is a monotypic species, endemic to México and only known from portions of the states of Coahuila, Zacatecas, and San Luis Potosí (Álvarez-Castañeda 2002). This species is sympatric with *P. eremicus, P. melanophrys*, and *P. pectoralis* in the states of Coahuila and Zacatecas (Schmidly *et al.* 1985). Its preferred habitat is the grassland transition zone, a mixture of desert scrub and grassland vegetation (Schmidly *et al.* 1985; Lee and Schmidly 1977). Its present fragmented and restricted distribution is considered a relict of a much larger historical distribution (Schmidly *et al.* 1985).

Peromyscus hooperi is poorly represented in mammal collections and little is known about its current status in their restricted distribution; however, it is not protected by the Mexican government (Norma Oficial Mexicana – 059 – 2020, Secretaría de Medio Ambiente y Recursos Naturales 2010) and is classified as Least Concern by the International Union for Conservation of Nature – IUCN – (accessed on August 2022, Álvarez-Castañeda 2016). The species resembles *P. eremicus*, *P. merriami*, and *P. pectoralis* in cranial and external characters but differs in the karyotype (Lee and Schmidly 1977; Schmidly *et al.* 1985). Fuller *et al.* (1984) and Schmidly *et al.* (1985) found that the karyotype of *P. hooperi* is very similar to *P. crinitus*, *P. simulus*, *Osgoodomys banderanus* and northern populations of *P. boylii*. However, *P. hooperi* has been described as a medium size mouse for the genus, with a long and bicolored tail (light grayish brown above and whitish below) with short hair. The upper parts, including face and top of head, are grayish with faint to moderate wash brown; lateral line is faint and near light buff; underparts are cream; and hind feet and lower legs are whitish. The skull contains large auditory bullae, and the first two upper and lower molars lack mesolophs. The glans penis is small but wide with a long protractile tip, and the baculum is long and slender with a cartilaginous tip (Lee and Schmidly 1977). The karyotype (2n = 48, FN = 52) comprises three pairs of biarmed autosomes and 20 pairs of acrocentric acrosomes (Lee and Schmidly 1977; Schmidly *et al.* 1985).

The taxonomic affinity of Hooper's deer mouse has been problematic (Carleton 1989). Based on a series of morphological characters (*i. e.,* cranial characteristics, accessory lophs, and styles of the anterior molars, structure of the hyoid, and number and placement of the mammae) it was suggested to be closely related to the subgenus *Haplomylomys* (Lee and Schmidly 1977). However, based on the anatomy of the phallus, it was more similar to species representing the subgenus *Peromyscus* (Lee and Schmidly 1977; Schmidly *et al.* 1985). Therefore, *P. hooperi* was characterized as an intermediate form between these two subgenera (Lee and Schmidly 1977; Fuller *et al.* 1984; Schmidly *et al.* 1985). *Peromyscus hooperi* currently is recognized as the sole member of the *Peromyscus hooperi* species group (Schmidly *et al.* 1985; Carleton 1989), based on morphological characters, karyotypes, allozymes, and mtDNA – cytochrome b (*Cytb;* Carleton 1989; Musser and Carleton 1993, 2005; Hogan *et al.* 1993; Dawson 2005; Bradley *et al.* 2007).

Bradley *et al.* (2007) used *Cytb* sequence data to conduct a phylogenetic analysis of the genus *Peromyscus*. They recovered strong nodal support for a sister group relationship between *P. hooperi* and *P. crinitus* with Maximum Parsimony (MP), however, using Maximum Likelihood (ML) and Bayesian Inference (BI) they did not resolve this relationship. In turn, this clade was sister to a clade including *P. melanotis, P. polionotus, P. maniculatus, P. keeni, P. leucopus, P. gossypinus, P. eremicus, P. californicus,* and *Osgoodomys banderanus*. Platt *et al.* (2015), included *Cytb* and three nuclear genes – *Adh1-I2*, *Fgb-I7* and *Rbp3*, and concluded that the phylogenetic position of *P. hooperi* remains uncertain due to a lack of support values and the different placement between ML and BI analyses.

An additional problem for the systematic classification of the species within *Peromyscus* is the very definition of the genus. Several revisions and classifications have recognized subgenera – *sensu lato* – (Osgood 1909; Hooper and Musser 1964; Hooper 1968) and genera – *sensu stricto* – (Carleton 1980; Carleton 1989; Musser and Carleton 2005) within *Peromyscus*. However, the current resolution of this group does not fully adhere to either of those classifications. In addition, genetic and genomic studies have demonstrated the paraphyly of *Peromyscus* (Bradley *et al.* 2007; Miller and Engstrom 2008; Platt *et al.* 2015; Sullivan *et al.* 2017; Castañeda-Rico *et al.* 2022). While clarifying the definition of *Peromyscus* is beyond the scope and objective of this manuscript, it is important to point out that whether we align to the *sensu lato* or *sensu stricto* classification of the genus, the phylogenetic placement of *P. hooperi* has not been well-resolved. However, hereafter, we recognized the genus *Peromyscus* as paraphyletic, including *Habromys, Megadontomys, Neotomodon, Osgoodomys,* and *Podomys* at the generic level (*sensu stricto*).

Uncertainty of the phylogenetic position of *P. hooperi* based on previous studies necessitates a revaluation using additional sequence data. To accomplish this, we used genome-wide data, including several thousand

nuclear ultraconserved elements and whole mitochondrial genomes from a museum voucher specimen of *P. hooperi* collected by Nelson and Goldman combined with data from previous studies. These data provide new evidence about the phylogenetic placement of *P. hooperi* and its time of divergence from other peromyscines.

Materials and methods

Sample collection and laboratory methods. We used a museum specimen sample of *Peromyscus hooperi* – USNM 79619 – (*ca.* 2 mm^2 of dry skin) deposited at the Smithsonian Institution's National Museum of Natural History; and collected by E. W. Nelson and E. A. Goldman on August 14, 1896 from Carneros, Coahuila, México. We followed strict protocols to avoid contamination during sampling, as described in McDonough *et al.* (2018) and Castañeda-Rico *et al.* (2020). All pre-PCR steps were performed in a laboratory dedicated to processing ancient and historical DNA at the Center for Conservation Genomics, Smithsonian National Zoo and Conservation Biology Institute, Washington, DC. A silica column extraction protocol (McDonough *et al.* 2018) was used to extract DNA. We quantified DNA with a Qubit 4 fluorometer (Thermo Fisher, Waltham, MA) using a 1x dsDNA HS assay and visualized DNA with a TapeStation 4200 System (Agilent Technologies, Santa Clara, CA) using High Sensitivity D1000 reagents. A dual-indexed library was prepared using the SRSLY PicoPlus NGS library prep kit (Claret Bioscience, LLC), according to the manufacturer's protocol. We performed dual indexing PCR with TruSeq-style indices (Meyer and Kircher 2010) using Kapa HiFi HotStart Uracil+ (Roche Sequencing), following the manufacturer's protocol. This library was amplified with 12 cycles of PCR. We then pooled three PCRs from the same library before cleaning to increase DNA fragment representation. We cleaned the indexed library using 1.6X solid-phased reversible immobilization (SPRI) magnetic beads (Rohland and Reich 2012), quantified concentration using a Qubit 4 fluorometer, and inspected size ranges and quality with a TapeStation 4200 System (conditions as mentioned above). Target-enrichment was performed to capture ultraconserved elements (UCE) and mitogenomes using the myBaits® UCE Tetrapods 5Kv1 kit (Daicel Arbor Biosciences) following the myBaits protocol v3, and the myBaits® Mito kit (Daicel Arbor Biosciences) for the house mouse *Mus musculus* panel, following the myBaits protocol v4. We amplified post-enrichment UCE and mitogenome libraries with 18 cycles of PCR using Kapa HiFi HotStart Ready Mix (Roche Sequencing), following the manufacturer's protocol. A 1.6X SPRI magnetic bead clean-up was performed subsequently. We again quantified and visualized the enriched libraries using a Qubit 4 fluorometer and a TapeStation 4200 System, respectively (conditions as mentioned above). Finally, captured libraries were sequenced on a partial lane of a NovaSeq 6000 SP PE 2 x 150 base pairs (bp; Illumina, Inc., San Diego, CA, US) at the Oklahoma Medical Research Foundation, Oklahoma City (combined with samples from unrelated projects).

In addition to the data generated in this study, we also reanalyzed previously published data including the following: UCEs and full mitogenomes from Castañeda-Rico *et al.* (2020, 2022), as well as *Cytb* gene sequences from Bradley *et al.* (2007), Platt *et al.* (2015), and Sullivan *et al.* (2017; Table 1 and Appendix 1).

Ultraconserved elements. We analyzed the raw data following the PHYLUCE v1.6.7 pipeline with the default parameters (Faircloth 2016 https://github.com/faircloth-lab/phyluce). Illumiprocessor 2.10 (Faircloth 2013) and Trim Galore 0.6.5 (https://github.com/FelixKrueger/TrimGalore) were used to trim adapters, barcode regions and low-quality bases. Reads were assembled into contigs using Trinity 2.8.5 (Grabherr *et al.* 2011), and identified contigs matching UCE loci in the 5K UCE probe set (https://github.com/faircloth-lab/uce-probe-sets). A monolithic FASTA file was produced to extract sequences from each sample. We aligned FASTA sequences using MAFFT 7.4 (Katoh and Standley 2013; Nakamura *et al.* 2018) and performed edge trimming. The resulting alignments were filtered to test them for various degrees of missing data (matrix completeness): 65 % matrix (35 % of the taxa missing for each UCE locus), 75 % matrix (25 % of taxa missing), 85 % matrix (15 % of taxa missing), 90 % matrix (10% of taxa missing), and 95 % matrix (5 % of taxa missing). Samples included in this dataset are shown in Table 1. We quantified informative sites with the PHYLUCE script *phyluce_align_get_informative_sites.py*. All of these analyses were performed on the Smithsonian Institution High Performance Computing Cluster (Smithsonian Institution, https://doi.org/10.25572/SIHPC).

We conducted a Maximum Likelihood (ML) analysis using RAxML 8.12 (Stamatakis 2014) with a GTRGAMMA site rate substitution model and 20 ML searches for the phylogenetic tree for each of the aforementioned data matrices (*i. e.,* 65 % to 95 % matrices). Nonparametric bootstrap replicates were generated using the -N autoMRE option which runs until convergence was reached. We reconciled the best fitting ML tree with the bootstrap replicate to obtain the final phylogenetic tree with support values using the -f b command.

We estimated the best evolutionary model of nucleotide substitution in jModelTest 2.1.1 (Guindon and Gascuel 2003; Darriba *et al.* 2012) using the Akaike Information Criterion (AIC). The TVW+G model was selected as the best fitting model with the following parameters: base frequencies A = 0.2988, C = 0.2013, G = 0.2026, T = 0.2972; nst = 6; and gamma shape = 0.1070. A Bayesian Inference analysis (BI) using MrBayes 3.2.6 (Huelsenbeck and Ronquist 2001; Ronquist and Huelsenbeck 2003) was performed on the 90 % matrix. The BI analyses comprised two independent runs with 50 million generations, sampling trees and parameters every 1,000 generations with four Markov-chains Monte Carlo (MCMC), three heated and one cold. We visualized output parameters using Tracer v1.7.1 (Rambaut *et al.* 2018) to check for convergence between runs and we discarded the first 25 % of the trees as burn-in.

A species tree analysis under the multispecies coalescent (MSC) model with ASTRAL-III v.5.7.8 (Zhang *et al.* 2018) was performed on the 90 % matrix. The local posterior probability – LPP – (Sayyari and Mirarab 2016) was used as branching support. We used the uce2speciestree pipeline script (Campana 2019 https://github.com/campanam/uce2speciestree) to generate input files for ASTRAL. This script uses RAxML to infer individual gene trees under the GTRGAMMA substitution model, and 100 bootstrap replicates.

Mitogenomes. FASTQ files were analyzed using FastQC v0.11.5 (Andrews 2010, www.bioinformatics.babraham.ac.uk/projects/fastqc). Adapter sequences and low-quality reads were removed using the default parameters (Phred:20, mean min-len:20) in Trim Galore 0.6.5 (https://github.com/FelixKrueger/TrimGalore). Exact duplicates were removed (-derep1,4) using Prinseq-lite v0.20.4 (Schmieder and Edwards 2011). We mapped the resulting high-quality reads to the closest available reference genome (*Peromyscus crinitus* – GenBank accession number KY707308), using the Geneious algorithm in Geneious Prime® 2021.2.2 (https://www.geneious.com) with default parameters (Medium-Low sensitivity, Maximum mismatches = 20 %, Maximum gaps = 10 %). A consensus sequence was generated with Geneious Prime® 2021.2.2 (https://www.geneious.com), using 4X as the lowest coverage to call a base, and aligned them using MAFFT 7.45 plug-in (Katoh and Standley 2013). We transferred annotations from the reference to rule out the presence of nuclear copies of mitochondrial genes (NUMTs), and translated all protein-coding genes to check for frame shifts or stop codons.

We aligned sequences with MAFFT 7.45 plug-in (Katoh and Standley 2013) in Geneious Prime® 2021.2.2 (https://www.geneious.com). Samples included in this dataset are listed in Table 1. A BI analysis was conducted on a partitioned dataset using MrBayes 3.2.6 (Huelsenbeck and Ronquist 2001; Ronquist and Huelsenbeck 2003). The best model and partition scheme were estimated using PartitionFinder 2.1.1 (Lanfear *et al.* 2016). Our search was limited to the models available in MrBayes, with linked, corrected Akaike Information Criterion (AICc) and greedy parameters. The data block was defined by gene, tRNA, rRNA and D-loop selection. We conducted two independent runs with 50 million generations, sampling trees and parameters every 1,000 generations with four MCMC and parameters as mentioned above, to perform the BI analysis. Convergence between runs was checked using Tracer v1.7.1 (Rambaut *et al.* 2018), and the first 25 % of the trees was discarded as burn-in.

We performed a ML analysis using the concatenated dataset in RAxML 8.12 (Stamatakis 2014) with a GTRGAMMA site rate substitution model. Clade support was assessed by bootstrapping with the -N autoMRE option for a bootstrap convergence criterion. The -f b option was used to reconcile the best fitting ML tree with the bootstrap rep-

Table 1. Specimens examined in this study using UCE and mitogenomes with species name, accession number collection/ID study (Smithsonian Institution's National Museum of Natural History USNM, Museum of Texas Tech University TK, and TTU associated, Museo de Zoología "Alfonso L. Herrera" Facultad de Ciencias UNAM MZFC, and University of Michigan Museum of Zoology –UMMZ), reference (the study from which the sequences were obtained or reanalyzed), GenBank BioProject, and GenBank accession numbers.

Species	Number Scientific Collection/ID	Reference	UCE (GenBank BioProject)	Mitogenome (GenBank number)
Peromyscus hooperi	USNM79619/USNM79619	This study	PRJNA880321	OP432689
Peromyscus boylii		This study		MZ433362
Peromyscus maniculatus		This study		MH260579
Peromyscus leucopus		This study		BK010700
Peromyscus megalops	USNM340233/USNM340233	Castañeda-Rico *et al.* (2022)	PRJNA838631	ON528115
Peromyscus attwateri	TTU143738/TK185663	Castañeda-Rico *et al.* (2022)	PRJNA838631	ON528112
Peromyscus aztecus	USNM569848/USNM569848	Castañeda-Rico *et al.* (2022)	PRJNA838631	ON528113
Peromyscus polionotus	USNM585473/USNM585473	Castañeda-Rico *et al.* (2022)	PRJNA838631	ON528117
Peromyscus crinitus	TTU146966/TK193714	Castañeda-Rico *et al.* (2022)	PRJNA838631	ON528114
Podomys floridanus	TTU97866/TK92501	Castañeda-Rico *et al.* (2022)	PRJNA838631	ON528118
Neotomodon alstoni	TTU82668/TK93098	Castañeda-Rico *et al.* (2022)	PRJNA838631	ON528110
Onychomys leucogaster	TTU146304/TK171574	Castañeda-Rico *et al.* (2022)	PRJNA838631	ON528111
Reithrodontomys mexicanus	TTU138428/TK178510	Castañeda-Rico *et al.* (2022)	PRJNA838631	ON528119
Isthmomys pirrensis	USNM565924/USNM565924	Castañeda-Rico *et al.* (2022)	PRJNA838631	ON528108
Neotoma mexicana	TTU104969/TK150189	Castañeda-Rico *et al.* (2022)	PRJNA838631	ON528109
Peromyscus mekisturus	UMMZ88967/UMMZ88967	Castañeda-Rico *et al.* (2020)	PRJNA606805	MT078818
Peromyscus melanophrys	MZFC3907/MQ1229	Castañeda-Rico *et al.* (2020)	PRJNA606805	MT078816
Peromyscus perfulvus	– /MCP119	Castañeda-Rico *et al.* (2020)	PRJNA606805	MT078817
Peromyscus pectoralis	MZFC10465/FCR176	Castañeda-Rico *et al.* (2020)	PRJNA606805	MT078819
Peromyscus mexicanus	MZFC11150/MRM030	Castañeda-Rico *et al.* (2020)	PRJNA606805	
Habromys simulatus	MZFC10104/HBR031	Castañeda-Rico *et al.* (2020)	PRJNA606805	

licate to obtain the final phylogenetic tree (as mentioned above). DNA damage patterns were evaluated for the *P. hooperi* sample with mapDamage2.0 (Jónsson *et al.* 2013) using -- rescale option.

Cytochrome b. We analyzed *Cytb* sequences extracted from the mitogenome that was generated in this study and from mitogenomes published by Sullivan *et al.* (2017) and Castañeda-Rico *et al.* (2020, 2022). We also used the *Cytb* sequences published by Bradley *et al.* (2007) and Platt *et al.* (2015) in order to compare the phylogenetic position of *P. hooperi* using genome-wide data as well as a single mitochondrial gene. The *Cytb* dataset allowed us to include more species within the genus *Peromyscus* and representatives of the genera *Habromys, Megadontomys, Neotomodon, Osgoodomys, Podomys, Isthmomys, Onychomys, Reithrodontomys, Neotoma, Ochrotomys, Baiomys, Ototylomys, Tylomys, Nyctomys, Oryzomys* and *Sigmodon*. Samples included in this dataset are shown in Table 1 and Appendix 1.

The *Cytb* dataset was analyzed as follows: we performed alignment using MAFFT 7.45 plug-in (Katoh and Standley 2013) in Geneious Prime® 2021.2.2 (https://www.geneious.com). We estimated the best evolutionary model of nucleotide substitution in jModelTest 2.1.1 (Guindon and Gascuel 2003; Darriba *et al.* 2012) using the AIC method. The TPM3uf+I+G model was selected as the best fitting model with the following parameters: base frequencies A = 0.3896, C = 0.3336, G = 0.0500, T = 0.2267; nst = 6; proportion of invariable sites = 0.4080; and gamma shape = 0.6220. A BI analysis was run using MrBayes 3.2.6 (Huelsenbeck and Ronquist 2001; Ronquist and Huelsenbeck 2003) as mentioned above for UCE and mitogenome datasets. We used Tracer v1.7.1 (Rambaut *et al.* 2018) to check for convergence between runs, and the first 25 % of the trees was discarded as burn-in.

Divergence times estimation. Molecular dates of divergence were estimated in BEAST2 v2.6.6 (Bouckaert *et al.* 2019) using the mitogenome dataset. First, we obtained the best model and partition scheme in PartitionFinder 2.1.1 (Lanfear *et al.* 2016). The search was limited to the models available in BEAST, linked branch lengths, AICc model selection, and greedy schemes search. The data block was defined by codon position, tRNA, rRNA and D-loop selection, and the result was incorporated in the dating analysis. The BEAST analysis was performed under an uncorrelated lognormal relaxed molecular clock model. The calibrated Yule speciation processes model (Heled and Drummond 2012) with a randomly generated starting tree were set up as priors. We used the same three calibration points with a lognormal distribution from Castañeda-Rico *et al.* (2022). Calibrations were based on fossil records of 1) *Reithrodontomys* (mean = 1.8 million years ago [mya], stdev = 1.076, offset = 1.63), as used by Steppan and Schenk (2017); 2) *Onychomys* (mean = 4.9, stdev = 1.169, offset = 4.753), as used by Steppan and Schenk (2017); and 3) the most recent common ancestor of *P. attwateri* (mean = 2.7, stdev = 0.9, offset = 2.4 [Dalquest 1962; Karow *et al.*1996; Wright *et al.* 2020]). Two independent runs of 50 million iterations were performed, each was sampled every 1,000 iterations. We checked convergence statistics for Effective Sample Sizes (ESS) using Tracer v1.7.1 (Rambaut *et al.* 2018) and a 25 % of burn-in was performed on each run. We used LogCombiner v2.6.6 to combine trees and TreeAnnotator v2.6.2 to get a consensus tree with node height distribution (both packages available in BEAST). All phylogenetic and ultrametric dated trees from the UCE, mitogenome and *Cytb* datasets were visualized in FigTree 1.4.4 (http://tree.bio.ed.ac.uk/software/figtree/). All analyses were performed on the Smithsonian Institution High Performance Computing Cluster (Smithsonian Institution https://doi.org/10.25572/SIHPC).

Results

Following the PHYLUCE v1.6.7 pipeline, we recovered 1,087 UCE loci (raw data are available in GenBank under BioProject PRJNA880321), and a complete mitogenome of 16,288 bp (GenBank accession number OP432689) from the *P. hooperi* sample. The average number of paired-end reads and fragment size after trimming were 13,075,112 reads and 67 bp long, respectively. The lowest-quality bases were detected at the end of the reads. We also recovered between 1,353 and 3,859 UCE loci from the reanalyzed samples. The average number of paired-end reads and fragment size after trimming for those samples ranged from 1,811,856 to 21,093,430 reads, and from 94 to 222 bp, respectively.

Ultraconserved Elements phylogenies. We recovered 9,840 contigs for *P. hooperi* after Trinity assemblies. The mean, minimum, and maximum length for contigs were 242, 201, and 3,784 bp, respectively. The incomplete matrix contained 4,406 UCE loci (*n* = 18, average = 3,136, min = 1,087, max = 3,859). A total of 1,087 UCE loci were obtained for *P. hooperi* with a mean, minimum, and maximum length of 235, 201, and 636 bp, respectively. The 65 % matrix contained 3,681 UCE loci (UL) with an average of 13.80 informative sites per locus (IS), the 75 % matrix (UL = 2,974, IS = 14.18, the 85 % matrix (UL = 1,514, IS = 14.29), the 90 % matrix (UL = 677, IS = 14.07), and the 95 % matrix (UL = 168, IS = 14.30).

The datasets representing various levels of matrix completeness yielded the same ML topology with high support values for all branches (Figure 1, phylogenetic trees obtained from the 65 %, 75 %, 85 %, and 95 % matrices are not shown). The BI tree topology, based on the 90 % matrix, showed the same topology with high posterior probability values for all branches (Figure 1). Both, ML and BI trees placed *P. hooperi* as sister to the clade containing *Podomys floridanus, Neotomodon alstoni, P. mexicanus*, *P. megalops*, *P. melanophrys*, *P. perfulvus*, *P. aztecus*, *Habromys simulatus*, *P. attwateri*, and *P. pectoralis*. The species tree supported, with high LPP values, the same phylogenic position of *P. hooperi* (Figure 1, based on the 90 % matrix). The only difference among the species tree and the concatenated ML and BI trees, was the relationship between *P. mexicanus* and

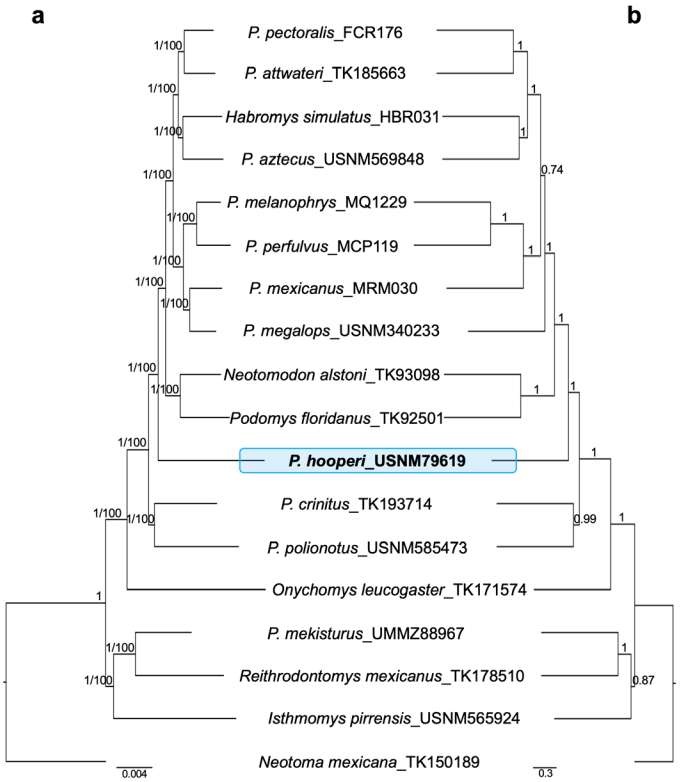

Figure 1. (a) Bayesian Inference and Maximum Likelihood phylogenies based on a 90 % matrix UCE with 677 loci. Nodal support is provided with posterior probability/bootstrap values. (b) Species tree based on a 90 % matrix UCE with 677 loci. Nodal support is provided with local posterior probability values. The blue block highlights the phylogenetic position of *Peromyscus hooperi*.

P. megalops. These two species are sisters in the ML and BI trees but not in the species tree, where *P. megalops* is sister to the clade containing *P. mexicanus*, *P. melanophrys, P. perfulvus, P. aztecus, Habromys simulatus, P. attwateri,* and *P. pectoralis*.

Mitogenome phylogenies. The final alignment included 21 taxa and was 16,272 bp in length. BI and ML analyses, with six partitions, provided slightly different topologies (Figure 2). However, both analyses supported (pp = 1, bootstrap = 76) the placement of *P. hooperi* as sister to the clade including *Podomys floridanus*, *Neotomodon alstoni*, *P. mexicanus*, *P. megalops*, *P. melanophrys*, *P. perfulvus*, *P. boylii*, *P. aztecus*, *Habromys ixtlani*, *P. attwateri*, and *P. pectoralis*. The phylogenetic position of *P. crinitus* changed across phylogenies (Figure 2), as did the position of the clade containing *Podomys floridanus* + *Neotomodon alstoni*. However, the BI tree yielded higher support values. The DNA damage analysis showed a weak signal of damage, typical of historical DNA (Appendix 2).

Cytochrome b phylogeny. The alignment included 64 taxa, 154 sequences, and was 1,143 bp in length. The BI analysis placed *P. hooperi* sister to the clade containing *P. maniculatus*, *P. polionotus*, *P. keeni*, *P. melanotis*, *P. leucopus*, and *P. gossypinus* (Appendix 3). However, the branch support value for this phylogenetic position was low (pp = 0.53). The two samples of *P. hooperi*, one sequenced in this study (USNM 79619) and the other by Bradley *et al.* (2007; TTU 104425, GenBank accession number DQ973103) clustered together with high support (pp = 1).

Divergence time estimation of Peromyscus hooperi. The mitochondrial divergence dating analysis, with six data partitions, estimated a Pliocene divergence time for *P. hooperi* around 3.98 mya (95 % HPD: 3.57 to 4.47 mya; Figure 3). The divergence of *P. crinitus* was dated *ca.* 4.31 mya (95 % HPD: 3.80 to 4.70 mya), the split of the clade including *P. leucopus* + (*P. polionotus* + *P. maniculatus*) at *ca.* 4.49 mya (95 % HPD: 4.03 – 5.02 mya), and the divergence of the genus *Peromyscus* was dated *ca.* 5.21 mya (95 % HPD: 4.79 – 5.71 mya).

Discussion

The biological expeditions undertaken by Nelson and Goldman in México were arguably among the most important ever achieved by two naturalists for a single country (López-Medellin and Medellin 2016; Guevara 2021; https://sova.si.edu/record/SIA.FARU7364). To our knowledge, this is one of a few studies in which genome-wide data were obtained and analyzed from a specimen collected by these two naturalists (see McDonough *et al.* 2022). Our results not only provide new evidence about the phylogenetic position of *P. hooperi* but also joins a short list of mammal studies within the blooming field of Museomics (see Card *et al.* 2021 for a review) that have successfully analyzed specimens collected before 1900 within a phylogeny (*e. g.*, Abreu-Jr *et al.* 2020; Sacks *et al.* 2021; Roycroft *et al.* 2021, 2022; Castañeda-Rico *et al.* 2022; McDonough *et al.* 2022; Tavares *et al.* 2022).

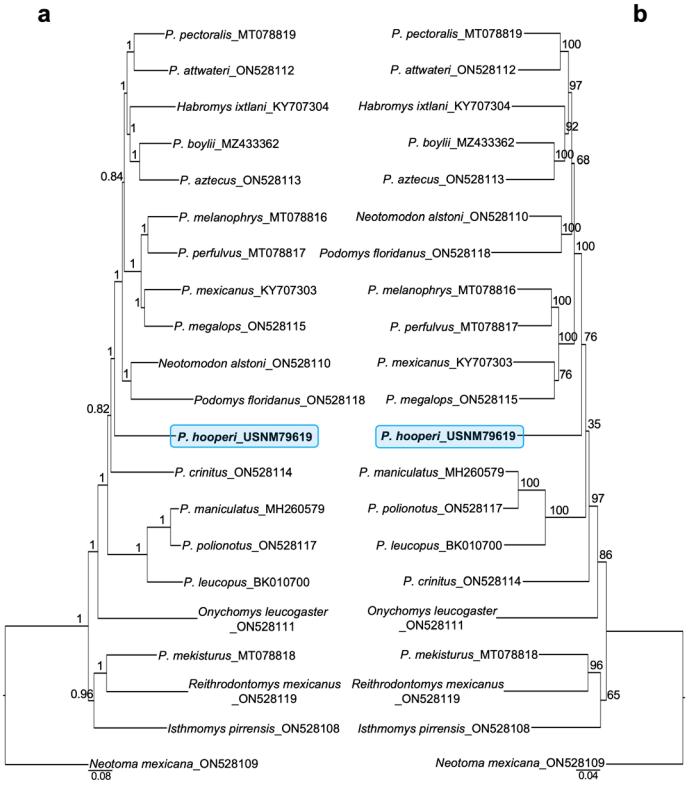

Figure 2. Mitogenome phylogenies based on Bayesian Inference (a) and Maximum Likelihood (b). Nodal support is provided with posterior probability and bootstrap values, respectively. The blue block highlights the phylogenetic position of *Peromyscus hooperi*.

Our nuclear DNA results strongly support *P. hooperi* as sister to a clade containing *Podomys floridanus*, *Neotomodon alstoni*, *Habromys simulatus*, *P. mexicanus*, *P. megalops*, *P. melanophrys*, *P. perfulvus*, *P. aztecus*, *P. attwateri*, and *P. pectoralis* (all *Peromyscus* species within the subgenus *Peromyscus*). In the mitogenome analyses, *P. boylii* (subgenus *Peromyscus*) and *H. ixtlani* joined the sister group of *P. hooperi* (Figure 1, 2). However, our results do not agree with those of Bradley *et al.* (2007), who found low support for *P. hooperi* as sister to *P. crinitus* (subgenus *Peromyscus*, *Peromyscus crinitus* species group), and both species sister to a clade including *P. melanotis*, *P. polionotus*, *P. maniculatus*, *P. keeni*, and *P. leucopus* (subgenus *Peromyscus*, *Peromyscus leucopus* and *maniculatus* species groups), *P. gossypinus*, *P. eremicus*, and *P. californicus* (subgenus *Haplomylomys*, *Peromyscus californicus* and *eremicus* species groups), and *Osgoodomys banderanus*. Platt *et al.* (2015) showed that *P. hooperi* could be related with the same species suggested by Bradley *et al.* (2007), although *P. polionotus* and *P. keeni* were not included in their study. However, the phylogenetic position of *P. hooperi* remained uncertain due to lack of strong nodal support in both of these previous studies.

Our phylogenomic analyses strongly support the placement of *P. hooperi* with the *Peromyscus mexicanus, megalops, aztecus, melanophrys*, and *truei* species groups (all within the subgenus *Peromyscus*). We did include three out of the five species groups studied by Bradley *et al.* (2007). We analyzed the only member of the *Peromyscus crinitus* species group in the nuclear and mitogenome dataset, and members of the *Peromyscus maniculatus* and *leucopus* species group only in the mitogenome dataset; but we did not find that *P. hooperi* is closely related to any of those groups as previously suggested. Despite the novel data generated here, denser taxon sampling is still required to better confirm and/or determine the closest relative of *P. hooperi*. For example, phylogenetic relationships between *P. hooperi* and members of the subgenus *Haplomylomys* still require further testing. However, despite this limitation, here we have provided strong nodal support for *P. hooperi* for the first time.

The *Cytb* analysis (Appendix 3) confirmed the identity of the *P. hooperi* specimen used in this study (USNM 79619), placing it in the same clade with the only other *P. hooperi* *Cytb* sequence available (Bradley *et al.* 2007, TTU 104425 and GenBank accession number DQ973103). In addition, the phylogenetic position of the species in this analysis is similar to Bradley *et al.* (2007) and Platt *et al.* (2015). We found that *P. hooperi* is most closely related to the *Peromyscus leucopus* and *maniculatus* species groups but with a low support (pp = 0.53); therefore, its phylogenetic posi-

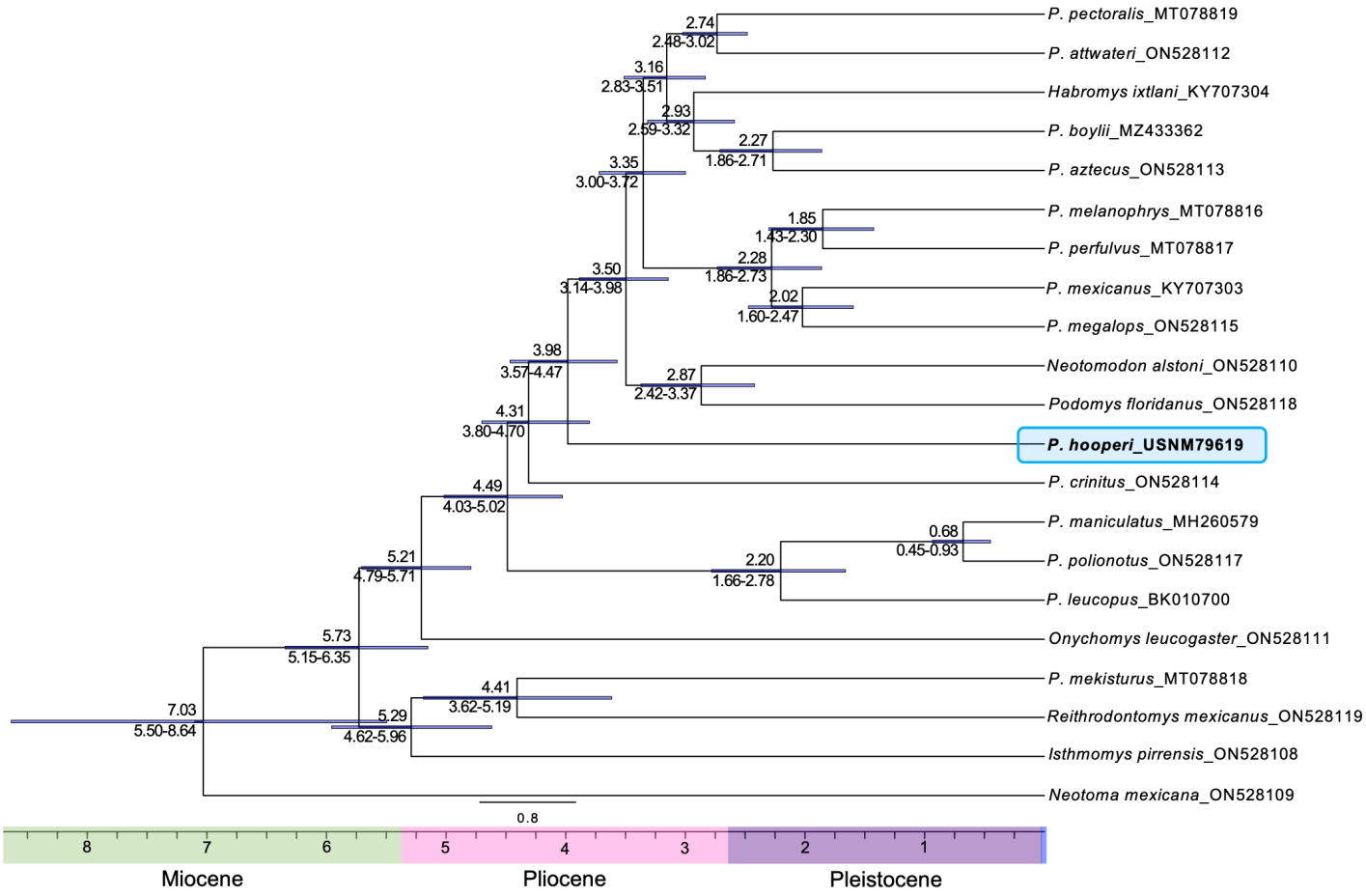

Figure 3. Dated whole mitochondrial genome phylogeny. Dates are provided in millions of years. The horizontal bars and numbers below the branches show the 95 % Highest Posterior Density. The blue block highlights the phylogenetic position of *Peromyscus hooperi*.

tion is not resolved. In conclusion, we confirmed that the phylogenetic position of the Hooper's deer mouse cannot be resolved using only *Cytb* sequences or a few genes, as Platt *et al.* (2015) documented. Our results demonstrate that genome-wide data allow a better resolution of the phylogenetic relationships of phylogenetically problematic species.

Our divergence times estimations indicated that the crown of *Peromyscus* was estimated *ca.* 5.21 mya (95 % HPD: 4.79 to 5.71 mya), and the diversification of the genus occurred *ca.* 4.49 mya (95 % HPD: 4.03 to 5.02 mya), both events during the Pliocene. We dated the split of *P. hooperi* during the Pliocene at *ca.* 3.98 mya (95 % HPD: 3.57 to 4.47 mya), following the split from *P. crinitus* at *ca.* 4.31 mya (95 % HPD: 3.80 to 4.70 mya). These dates coincide with previously dated phylogenies obtained from genome-wide data of peromyscines (*e. g.,* Castañeda-Rico *et al.* 2022). They estimated the crown of the genus *Peromyscus* during the Pliocene at *ca.* 5.32 mya (95 % HPD: 4.85 to 5.98 mya), and the origin of *P. crinitus* at *ca.* 4.62 mya (95 % HPD: 4.05 to 5.28 mya), using mitogenomes. Our results also show that the *Peromyscus hooperi*, *crinitus*, *maniculatus*, and *leucopus* species groups were among the first to diverge within the genus *Peromyscus* (Figure 3), followed by the *Peromyscus megalops, mexicanus*, *melanophrys*, *boylii*, *aztecus,* and *truei* species groups, together with *Neotomodon, Podomys*, and *Habromys*. Based on our results and those of previous studies (*e. g.,* Hibbard 1968; Riddle *et al.* 2000; Dawson 2005; Castañeda-Rico *et al.* 2014, 2022; Platt *et al.* 2015; Sawyer *et al.* 2017; León-Tapia *et al.* 2021), we suggest the Pliocene and Pleistocene as the time when speciation and diversification events took place within peromyscines, potentially associated with climatic cycles related to numerous vicariant and dispersal events.

Previous phylogenetic studies of the genus *Peromyscus* that analyzed single or few genes, provided older divergence times estimations (*e. g.,* Castañeda-Rico *et al.* 2014; Platt *et al.* 2015; Cornejo-Latorre *et al.* 2017; Bradley *et al.* 2019). For example, Platt *et al.* (2015), using *Cytb*, estimated the origin of *Peromyscus* and its diversification, during the Miocene, at approximately 8 mya and 5.71 mya, respectively; and the divergence of *P. hooperi* at *ca.* 5.2 mya, during the early Pliocene. However, estimates of the time to the most recent common ancestor (TMRCA) calculated from individual or few genes can be overestimated (Duchêne *et al.* 2011).

The evolutionary uniqueness of *P. hooperi* is supported by our results and previous studies by Fuller *et al.* (1984) and Schmidly *et al.* (1985) who found that this species does not fit well with either of the subgenera *Haplomylomys* or *Peromyscus*. We hypothesize that *P. hooperi* will remain the sole member of the *Peromyscus hooperi* group as first proposed by Schmidly *et al.* (1985) and later supported by Carleton (1989) based on the morphological, karyotypic, and allozyme evidence.

The genetic and morphological uniqueness of *P. hooperi*, as well as its restricted distribution to grassland transition zones should make this a species of special concern for conservation. In addition, Schmidly *et al.* (1985) stated that *P. hooperi* is a relictual, monotypic species without close living relatives, and its survival is jeopardized/threatened by the fragile conditions of its habitat in central Coahuila as a result of overgrazing. During the last 21 years, habitat shifts from native grasslands to crops zones have increased with agricultural intensification, grain-fed cattle feedlots, and new land use policies in the Mexican states of Durango, Sinaloa, Chihuahua, Nuevo León, and particularly Coahuila where *P. hooperi* is mostly distributed (Galván-Miyoshi *et al.* 2015; Bonilla-Moheno and Aide 2020). We recommend that future studies conduct population genetic analyses to determine the genetic diversity and structure of the different populations of *P. hooperi*. This species remains poorly known and potentially threatened by habitat loss, therefore new information is needed to determine an appropriate conservation strategy and category.

Acknowledgements

We wish to specially thank the specimen collectors, collection managers, curators and all museum staff of the Smithsonian Institution's National Museum of Natural History (NMNH) that granted the destructive sampling of the *Peromyscus hooperi* museum specimen; and the Museum of Texas Tech University (TTU), the University of Michigan Museum of Zoology (UMMZ), and the Museo de Zoología "Alfonso L. Herrera", Facultad de Ciencias, UNAM (MZFC) that granted previous sample loans. We also would like to thank the Associate Editor and two anonymous reviewers that provided comments that greatly improved the quality of this manuscript.

This manuscript is dedicated to Dr. Alfred L. Gardner (Al) for his significant contributions to the field Mammalogy through his numerous publications, research, and teachings, especially for the long-lasting impact that he has made on Mexican Mammalogy. We sincerely thank him for his invaluable help and enthusiasm to support students, researchers, and colleagues not only from Latin America but from all around the world.

Literature cited

Abreu-Jr., E. F., *et al.* 2020. Museomics of tree squirrels: a dense taxon sampling of mitogenomes reveals hidden diversity, phenotypic convergence, and the need of a taxonomic overhaul. BMC Evolutionary Biology 20:77.

Andrews, S. 2010. FastQC: A Quality Control Tool For High Throughput Sequence Data. http://www.bioinformatics.babraham.ac.uk/projects/ fastqc

Álvarez-Castañeda, S. T. 2002. *Peromyscus hooperi*. Mammalian Species 709:1–3.

Álvarez-Castañeda, S. T. 2016. *Peromyscus hooperi*. in IUCN 2022. The IUCN Red List of Threatened Species. Version 2022-1. www.iucnredlist.org Accessed on 22 August 2022.

Bonilla-Moheno, M., and T. M. Aide. 2020. Beyond deforestation: Land cover transition in Mexico. Agricultural System 178:102734.

Bradley, R. D., *et al*. 2007. Toward a molecular Phylogeny for *Peromyscus*: evidence from mitochondrial cytochrome-b sequences. Journal of Mammalogy 88:1146–1159.

Bradley, R. D., *et al*. 2019. Mitochondrial DNA sequence data indicate evidence for multiple species within *Peromyscus maniculatus*. Special Publications Museum of Texas Tech University 70:1–68.

Bouckaert, R., *et al*. 2019. BEAST 2.5: An advanced software platform for Bayesian evolutionary analysis. PLoS Computational Biology 15:e1006650.

Campana, M. G. 2019. uce2speciestree. https://github.com/campanam/uce2speciestree. Accessed on 22 August 2022.

Card, D. C., *et al*. 2021. Museum Genomics. Annual Review of Genetics 55:633–659.

Carleton, M. D. 1980. Phylogenetic relationships in Neotomine– Peromyscine rodents (Muridae) and a reappraisal of the dichotomy within New World Cricetinae. Miscellaneous Publications of the Museum of Zoology, University of Michigan 157:1–146.

Carleton, M. D. 1989. Systematics and evolution. Pp. 7–141, *in* Advances in the study of *Peromyscus* (Rodentia) (G. L. Kirkland, Jr. and J. N. Layne, eds.). Texas Tech University Press, Lubbock, USA.

Castañeda-Rico, S., *et al*. 2014. Evolutionary diversification and speciation in rodents of the Mexican lowlands: the *Peromyscus melanophrys* species group. Molecular Phylogenetics and Evolution 70:454–463.

Castañeda-Rico, S., *et al*. 2020. Ancient DNA From Museum Specimens and Next Generation Sequencing Help Resolve the Controversial Evolutionary History of the Critically Endangered Puebla Deer Mouse. Frontiers in Ecology and Evolution 8:94.

Castañeda-Rico, S., *et al*. 2022. Museomics and the holotype of a critically endangered cricetid rodent provide key evidence of an undescribed genus. Frontiers in Ecology and Evolution 10:930356.

Cornejo-Latorre, C., *et al*. 2017. The evolutionary history of the subgenus *Haplomylomys* (Cricetidae: *Peromyscus*). Journal of Mammalogy 98:1627-1640.

Dalquest, W. W. 1962. The Good Creek formation, Pleistocene of Texas, and its fauna. Journal of Paleontology 36:568–582.

Darriba, D., *et al*. 2012. jModelTest 2: more models, new heuristics and parallel computing. Nature Methods 9:772.

Dawson, W. 2005. Peromyscine biogeography, Mexican topography and Pleistocene climatology. Pp. 145–156, *in* Contribuciones Mastozoológicas en Homenaje a Bernardo Villa (V. Sánchez-Cordero and R. Medellín, eds.). UNAM-CONABIO, Ciudad de México, México.

Duchêne, S., *et al*. 2011. Mitogenome phylogenetics: The impact of using single regions and partitioning schemes on topology, substitution rate and divergence time estimation. PLoS ONE. 6:e27138.

Faircloth, B. C. 2013. Illumiprocessor: a Trimmomatic wrapper for parallel adapter and quality trimming. doi: 10.6079/J9ILL

Faircloth, B. C. 2016. PHYLUCE is a software package for the analysis of conserved genomic loci. Bioinformatics 32:786–788.

Fuller, B., *et al*. 1984. Albumin evolution in *Peromyscus* and *Sigmodon*. Journal of Mammalogy 65:466–473.

Galván-Miyoshi, Y., *et al*. 2015. Land Change Regimes and the Evolution of the Maize-Cattle Complex in Neoliberal Mexico. Land 4:754–777.

Grabherr, M. G., *et al*. 2011. Full-length transcriptome assembly from RNA-seq data without a reference genome. Nature Biotechnology 29:644–652.

Guevara, L. The legacy of the fieldwork of E. W. Nelson and E. A. Goldman in Mexico (1892–1906) for research on poorly known mammals. 2021. History and Philosophy of the Life Sciences 43:31.

Guindon, S., and O. Gascuel. 2003. A simple, fast and accurate method to estimate large phylogenies by maximum-likelihood. Systematic Biology 52:696–704.

Heled, J., and A. J. Drummond. 2012. Calibrated tree priors for relaxed phylogenetics and divergence time estimation. Systematic Biology 61:138–149.

Hibbard, C.W. 1968. Paleontology. Pp. 6–26, *in* Biology of *Peromyscus* (Rodentia) (King, J. A., ed.). Special Publication 2, American Society of Mammalogist, Oklahoma, USA.

Hogan, K., *et al*. 1993. Systematic and taxonomic implications of karyotypic, electrophoretic and mitochondrial DNA variation in *Peromyscus* from the Pacific Northwest. Journal of Mammalogy 74:819–831.

Hooper, E. T. 1968. Classification. Pp. 27–74, *in* Biology of *Peromyscus* (Rodentia) (J. A. King, ed.). Special Publication 2, The American Society of Mammalogists, Oklahoma, USA.

Hooper, E. T., and G. G. Musser. 1964. Notes on classification of the rodent genus *Peromyscus*. Occasional Papers of the Museum of Zoology, University of Michigan 635:1–13.

Huelsenbeck, J. P., and F. Ronquist. 2001. MRBAYES: bayesian inference of phylogeny. Bioinformatics 17:754–755.

Jónsson, H., *et al*. 2013. mapDamage2.0: fast approximate Bayesian estimates of ancient DNA damage parameters. Bioinformatics 13:1682–1684.

Karow, P. F., *et al*. 1996. Middle Pleistocene (early Rancholabrean) vertebrates and associated marine and non-marine invertebrates from Oldsmar, Pinellas County, Florida. Pp. 97–133, *in* Palaeoecology and palaeoenvironments of Late Cenozoic mammals: Tributes to the career of C. S. (Rufus) Churcher (K. Stewart and K. Seymour, eds.). University of Toronto Press, Toronto, Canada.

Katoh, K., and D. M. Standley. 2013. MAFFT multiple sequence alignment software version 7: improvements in performance and usability. Molecular Biology and Evolution 30:772–780.

Lanfear, R., *et al*. 2016. PartitionFinder 2: new methods for selecting partitioned models of evolution for molecular and morphological phylogenetic analyses. Molecular Biology and Evolution 34:772–773.

Lee, M. R., and D. J. Schmidly. 1977. A new species of *Peromyscus* (Rodentia: Muridae) from Coahuila, Mexico. Journal of Mammalogy 58:263–268.

León-Tapia, M.A., *et al*. 2021. Role of Pleistocene climatic oscillations on genetic differentiation and evolutionary history of the Transvolcanic deer mouse *Peromyscus hylocetes* (Rodentia: Cricetidae) throughout the Mexican central highlands. Journal of Zoological Systematics and Evolutionary Research 59:2481-2499.

López-Medellín, X., and R. Medellín. 2016. The influence of E. W. Nelson and E. A. Goldman on Mexican Mammalogy. Special Publications Museum of Texas Tech University 64:87–103.

McDonough, M. M., *et al*. 2018. Performance of commonly requested destructive museum samples for mammalian genomic studies. Journal of Mammalogy 99:789–802.

McDonough, M. M., *et al*. 2022. Phylogenomic systematics of the spotted skunks (Carnivora, Mephitidae, Spilogale): Additional species diversity and Pleistocene climate change as a major driver of diversification. Molecular Phylogenetic and Evolution 167:107266.

Meyer, M., and M. Kircher. 2010. Illumina sequencing library preparation for highly multiplexed target capture and sequencing. Cold Spring Harbor Protocols 2010:pdb.prot5448.

Miller, J. R., and M. D. Engstrom. 2008. The relationships of major lineages within peromyscine rodents: a molecular phylogenetic hypothesis and systematic reappraisal. Journal of Mammalogy 89:1279–1295.

Musser, G., and M. D. Carleton. 1993. Family Muridae. Pp. 501–755, *in* Mammal Species of the World: A Taxonomic and Geographic Reference (Wilson, D. E., and M. Reeder, eds.). Smithsonian Institution Press, Washington DC, USA.

Musser, G., and M. D. Carleton. 2005. Superfamily Muridae. Pp. 894–1531, *in* Mammal Species of the World: A Taxonomic and Geographic Reference (Wilson, D. E., and M. Reeder, eds.). Johns Hopkins University Press, Baltimore, USA.

Nakamura, T., *et al*. 2018. Parallelization of MAFFT for large-scale multiple sequence alignments. Bioinformatics 34:2490–2492.

Osgood, W. H. 1909. Revision of the mice of the American genus *Peromyscus*. North American Fauna 28:1–285.

Platt, R. N. II., *et al*. 2015. What is *Peromyscus*? Evidence from nuclear and mitochondrial DNA sequences suggests the need for a new classification. Journal of Mammalogy 96:708–719.

Rambaut, A., *et al*. 2018. Posterior summarization in Bayesian phylogenetics using Tracer 1.7. Systematic Biology 67:901–904.

Riddle, B., *et al*. 2000. Phylogeography and Systematics of the *Peromyscus eremicus* species group and the historical biogeography of North American Warm Regional deserts. Molecular Phylogenetics and Evolution 17:145–160.

Rohland, N., and D. Reich. 2012. Cost-effective, high-throughput DNA sequencing libraries for multiplexed target capture. Genome Research 22:939–946.

Ronquist, F., and J. P. Huelsenbeck. 2003. MRBAYES 3: bayesian phylogenetic inference under mixed models. Bioinformatics 19:1572–1574.

Roycroft, E., *et al*. 2021. Museum genomics reveals the rapid decline and extinction of Australian rodents since European settlement. Proceedings of the National Academy of Sciences 118:e2021390118.

Roycroft, E., *et al*. 2022. Sequence capture from historical museum specimens: maximizing value for population and phylogenomic studies. Frontiers in Ecology and Evolution 10:931644.

Sacks, B. N., *et al*. 2021. Pleistocene origins, western ghost lineages, and the emerging phylogeographic history of the red wolf and coyote. Molecular Ecology 30:4292-4304.

Schimidly, D. J., *et al*. 1985. Systematics and notes on the biology of *Peromyscus hooperi*. Occasional Papers, Museum of Texas Tech University 97:1–40.

Schmieder, R., and R. Edwards. 2011. Quality control and preprocessing of metagenomic datasets. Bioinformatics 27:863–864.

Secretaría de Medio Ambiente y Recursos Naturales. 2010. Norma Oficial Mexicana NOM-059-SEMARNAT-2010, Protección ambiental–Especies nativas de México de flora y fauna silvestres–Categorías de riesgo y especificaciones para su inclusión, exclusión o cambio–Lista de especies en riesgo. Diario Oficial de la Federación. México. 30 de diciembre de 2010.

Sawyer, Y. E., *et al*. 2017. Diversification of deermice (Rodentia: genus *Peromyscus*) at their north- western range limit: genetic consequences of refugial and island isolation. Journal of Biogeography 44:1572-1585.

Sayyari, E., and S. Mirarab. 2016. Fast coalescent-based computation of local branch support from quartet frequencies. Molecular Biology and Evolution 33:1654–1668.

Stamatakis, A. 2014. RAxML Version 8: a tool for phylogenetic analysis and post-analysis of large phylogenies. Bioinformatics 30:1312–1313.

Steppan, S., and J. J. Schenk. 2017. Muroid rodent phylogenetics: 900-species tree reveals increasing diversification rates. PLoS ONE 12:e0183070.

Sullivan, K. A. M., *et al*. 2017. Whole mitochondrial genomes provide increased resolution and indicate paraphyly in deer mice. BMC Zoology 2:11.

Tavares, V.C., *et al*. 2022. Historical DNA data of rare Yellow-eared bats *Vampyressa* Thomas, 1900 (Chiroptera, Phyllostomidae) clarifies phylogeny and species boundaries within the genus. Systematics and Biodiversity 20:1.

Wright, E. A., *et al*. 2020. Evidence from mitochondrial DNA sequences suggest a recent origin for *Peromyscus truei comanche*. Occasional Papers Texas Tech University Museum 367:1–19.

Zhang C., *et al*. 2018. ASTRAL-III: Polynomial time species tree reconstruction from partially resolved gene trees. BMC Bioinformatics 19:15–30.

Associated editor: Jake Esselstyn and Giovani Hernández Canchola
Submitted: September 12, 2022; Reviewed: October 25, 2022
Accepted: November 30, 2022; Published on line: January 27, 2023

Appendix 1

Specimens examined in this study using *Cytb* gene. We show the name of the species, reference (the study from which the sequences were obtained or reanalyzed), and GenBank accession number.

Species	Study	Mitogenome (GenBank number)	*Cytb* (GenBank number)
Onychomys leucogaster	Castañeda-Rico *et al.* (2020)	KU168563 (To extract *Cytb*)	
Habromys ixtlani	Sullivan *et al.* (2017)	KY707304 (To extract *Cytb*)	
Isthmomys pirrensis	Sullivan *et al.* (2017)	KY707312 (To extract *Cytb*)	
Neotoma mexicana	Sullivan *et al.* (2017)	KY707300 (To extract *Cytb*)	
Neotomodon alstoni	Sullivan *et al.* (2017)	KY707310 (To extract *Cytb*)	
Peromyscus attwateri	Sullivan *et al.* (2017)	KY707299 (To extract *Cytb*)	
Peromyscus aztecus	Sullivan *et al.* (2017)	KY707306 (To extract *Cytb*)	
Peromyscus crinitus	Sullivan *et al.* (2017)	KY707308 (To extract *Cytb*)	
Peromyscus megalops	Sullivan *et al.* (2017)	KY707305 (To extract *Cytb*)	
Peromyscus mexicanus	Sullivan *et al.* (2017)	KY707303 (To extract *Cytb*)	
Peromyscus pectoralis	Sullivan *et al.* (2017)	KY707309 (To extract *Cytb*)	
Peromyscus polionotus	Sullivan *et al.* (2017)	KY707301 (To extract *Cytb*)	
Podomys floridanus	Sullivan *et al.* (2017)	KY707302 (To extract *Cytb*)	
Reithrodontomys mexicanus	Sullivan *et al.* (2017)	KY707307 (To extract *Cytb*)	
Sigmodon hispidus	Sullivan *et al.* (2017)	KY707311 (To extract *Cytb*)	
Baiomys taylori	Bradley *et al.* (2007)		AF548469
Habromys ixtlani	Bradley *et al.* (2007)		DQ861395
			DQ000482
Habromys ixtlani	Bradley *et al.* (2007)		DQ973099
Isthmomys pirrensis	Bradley *et al.* (2007)		DQ836299
Megadontomys cryophilus	Bradley *et al.* (2007)		DQ861373
Megadontomys thomasi	Bradley *et al.* (2007)		AY195795
Neotoma mexicana	Bradley *et al.* (2007)		AF294345
Neotomodon alstoni	Bradley *et al.* (2007)		AY195796
			AY195797
			DQ861374
Nyctomys sumichrasti	Bradley *et al.* (2007)		AY195801
Ochrotomys nuttalli	Bradley *et al.* (2007)		AY195798
Onychomys arenicola	Bradley *et al.* (2007)		AY195793
Oryzomys palustris	Bradley *et al.* (2007)		DQ185382
Osgoodomys banderanus	Bradley *et al.* (2007)		AF155383
			DQ000473
Ototylomys phyllotis	Bradley *et al.* (2007)		AY009789
Peromyscus attwateri	Bradley *et al.* (2007)		AF155384
			AF155385
Peromyscus aztecus	Bradley *et al.* (2007)		U89968
Peromycus beatae	Bradley *et al.* (2007)		AF131921
			AF131922
			AF131914
Peromyscus boylii	Bradley *et al.* (2007)		AF155386
			AF155392
			AF155388
Peromyscus californicus	Bradley *et al.* (2007)		AF155393
Peromyscus crinitus	Bradley *et al.* (2007)		AY376413
			DQ861378
Peromyscus crinitus	Bradley *et al.* (2007)		EF028168
Peromyscus difficilis	Bradley *et al.* (2007)		AY376419 AY376415
			AY387488

Appendix 1
Continuation

Species	Study	Mitogenome (GenBank number)	*Cytb* (GenBank number)
Peromyscus eremicus	Bradley *et al.* (2007)		AY195799
			AY322503
Peromyscus eremicus	Bradley *et al.* (2007)		DQ973100
Peromyscus evides	Bradley *et al.* (2007)		U89970
Peromyscus furvus	Bradley *et al.* (2007)		AF271032
			AF271012
			AF271005
Peromycus gossypinus	Bradley *et al.* (2007)		DQ973101
			DQ973102
Peromyscus gratus	Bradley *et al.* (2007)		AY322507
			AY376421
			AY376422
Peromyscus guatemalensis	Bradley *et al.* (2007)		EF028171
			EF028172
Peromyscus gymnotis	Bradley *et al.* (2007)		EF028169
			EF028170
			EF028169
Peromyscus hooperi	Bradley *et al.* (2007)		DQ973103
Peromyscus hylocetes	Bradley *et al.* (2007)		U89976
			DQ000481
Peromyscus keeni	Bradley *et al.* (2007)		X89787
			AF119261
Peromyscus leucopus	Bradley *et al.* (2007)		AF131926
			DQ000483
Peromyscus leucopus	Bradley *et al.* (2007)		DQ973104
Peromyscus levipes	Bradley *et al.* (2007)		AF131928
			AY322509
			AF155396
Peromyscus madrensis	Bradley *et al.* (2007)		AF155397
Peromyscus maniculatus	Bradley *et al.* (2007)		DQ000484
			AY322508
Peromyscus maniculatus	Bradley *et al.* (2007)		DQ973111
Peromyscus mayensis	Bradley *et al.* (2007)		DQ836300
			DQ836301
Peromyscus megalops	Bradley *et al.* (2007)		DQ000475
Peromyscus melanocarpus	Bradley *et al.* (2007)		EF028173
Peromyscus melanophrys	Bradley *et al.* (2007)		AY322510
			AY376424
Peromyscus melanophrys	Bradley *et al.* (2007)		DQ973105
Peromyscus melanotis	Bradley *et al.* (2007)		AF155398
Peromyscus mexicanus	Bradley *et al.* (2007)		AY376425
Peromyscus mexicanus	Bradley *et al.* (2007)		EF028174
Peromyscus nasutus	Bradley *et al.* (2007)		AF155399
			AY376426
Peromyscus nudipes	Bradley *et al.* (2007)		AY041200
Peromyscus oaxacensis	Bradley *et al.* (2007)		U89972
Peromyscus ochraventer	Bradley *et al.* (2007)		DQ973106

Appendix 1
Continuation

Species	Study	Mitogenome (GenBank number)	*Cytb* (GenBank number)
Peromyscus pectoralis	Bradley *et al.* (2007)		AF155400
			AY322511
			AY376427
Peromyscus perfulvus	Bradley *et al.* (2007)		DQ000474
Peromyscus polionotus	Bradley *et al.* (2007)		X89792
Peromyscus polius	Bradley *et al.* (2007)		AF155403
Peromyscus sagax	Bradley *et al.* (2007)		AF155404
Peromyscus schmidlyi	Bradley *et al.* (2007)		AY322520
			AF155405
			AY370610
Peromyscus simulus	Bradley *et al.* (2007)		AF131927
Peromyscus spicilegus	Bradley *et al.* (2007)		AY322512
			DQ000480
Peromyscus spicilegus	Bradley *et al.* (2007)		DQ973107
Peromyscus stephani	Bradley *et al.* (2007)		AF155411
Peromyscus stirtoni	Bradley *et al.* (2007)		DQ973108
Peromyscus truei	Bradley *et al.* (2007)		AY376433
			AF108703
			AY376428
Peromyscus winkelmanni	Bradley *et al.* (2007)		AF131930
			U89983
Peromyscus zarhynchus	Bradley *et al.* (2007)		AY195800
Podomys floridanus	Bradley *et al.* (2007)		DQ973109
			DQ973110
Reithrodontomys megalotis	Bradley *et al.* (2007)		AF176248
Reithrodontomys mexicanus	Bradley *et al.* (2007)		AY859447
Sigmodon hispidus	Bradley *et al.* (2007)		AF155420
Tylomys nudicaudatus	Bradley *et al.* (2007)		AF307839
Isthmomys pirrensis	Platt II *et al.* (2015)		FJ214681
Peromyscus crinitus	Platt II *et al.* (2015)		FJ214684
Peromyscus eremicus	Platt II *et al.* (2015)		AY322503
Peromyscus evides	Platt II *et al.* (2015)		FJ214685
Peromyscus levipes	Platt II *et al.* (2015)		DQ000477
Peromyscus mexicanus	Platt II *et al.* (2015)		JX910118
Peromyscus nudipes	Platt II *et al.* (2015)		FJ214687
Peromyscus ochraventer	Platt II *et al.* (2015)		JX910119
Peromyscus spicilegus	Platt II *et al.* (2015)		FJ214669
Reithrodontomys fulvescens	Platt II *et al.* (2015)		AF176257
Reithrodontomys sumichrasti	Platt II *et al.* (2015)		AF176256
Reithrodontomys mexicanus	Platt II *et al.* (2015)		AY859453

Appendix 2

Comparison of C → T terminal deamination patters of *Peromyscus hooperi* (USNM 79619).

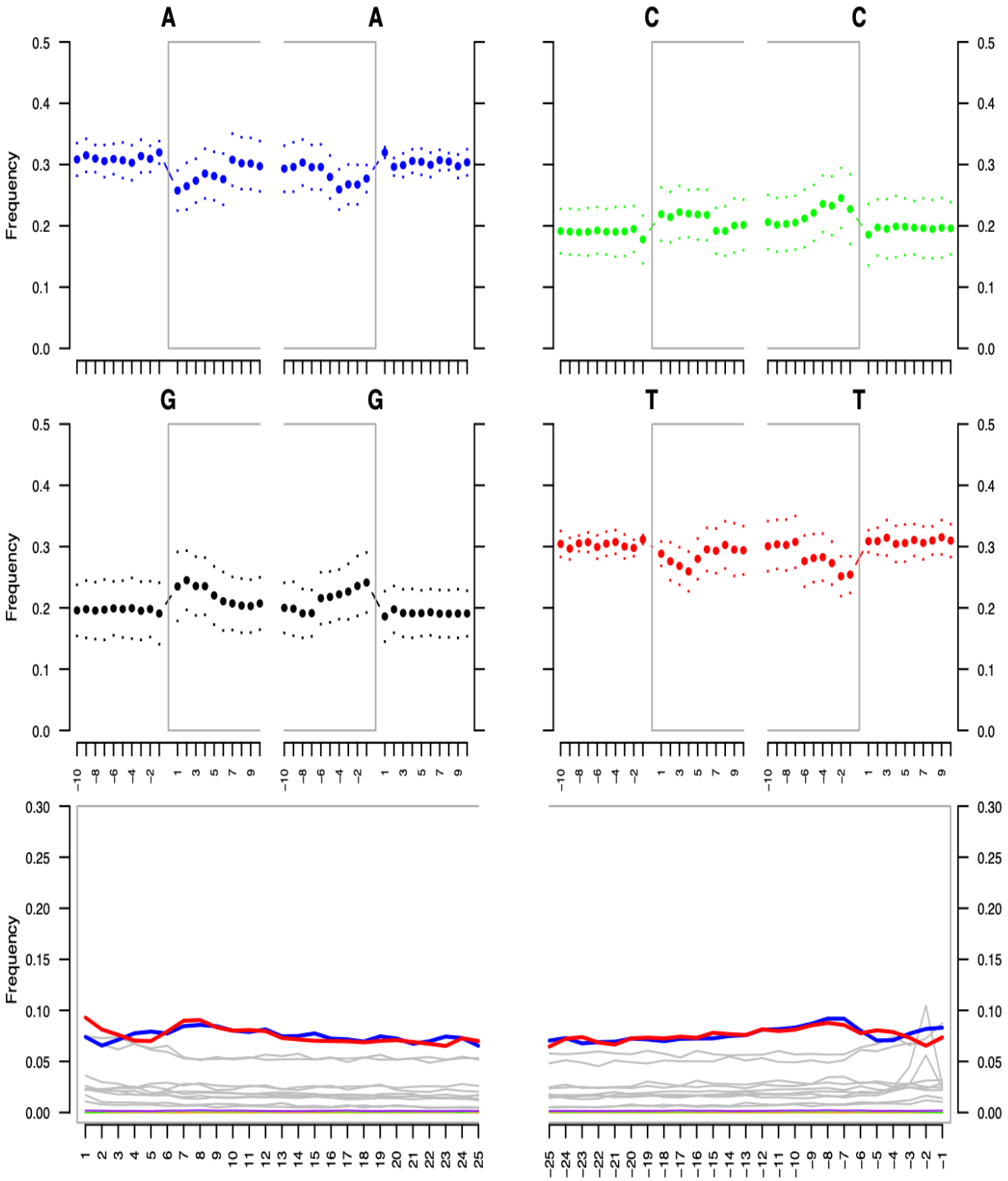

Appendix 3

Bayesian phylogenetic tree based on mtDNA *Cytb* sequence data. Nodal support is provided with posterior probability values. The blue block highlights the phylogenetic position of *Peromyscus hooperi*.